CrossMark

# Effect of Ba²⁺ doping on microstructure and electric properties of calcium copper titanate (CaCu₃Ti₄O₁₂) ceramics

Shuang Wu[1] · Pei Liu[1,2] · Yuanming Lai[1,3] · Weiming Guan[1] · Zihan Huang[1] ·
Jiao Han[1] · Yao Xiang[1] · Wei Yi[1] · Yiming Zeng[1]

**Abstract** The Ba²⁺ doped ceramics of $Ca_{1-x}Ba_xCu_3Ti_4O_{12}$ (x = 0.005, 0.01, 0.03, 0.05 and 0.1) were sintered via conventional solid-state reaction at 1050 °C for 8 h in air. The microstructure and electric properties of Ba²⁺ doping ceramics were investigated. The lattice parameters of $Ca_{1-x}Ba_xCu_3Ti_4O_{12}$ (CBCTO) ceramics decreased with the Ba²⁺ doping, and $Ba_{1.31}Ti_8O_{16}$ as secondary phase was confirmed at x = 0.1. The doping of Ba²⁺ resulted in uniformly distribution of small size grain (∼ 4 μm). All the doped samples showed lower value of dielectric constant than $CaCu_3Ti_4O_{12}$ (CCTO), due to low resistivity of the grain boundary with the Ba²⁺ doped samples. The nonlinear coefficient and breakdown field were significantly enhanced by Ba²⁺ doping.

## 1 Introduction

Since the giant dielectric properties of CCTO were found by Subramanian et al. in 2000, researchers paid lots of attentions on CCTO for its giant dielectric constant (over $10^5$) and temperature-independent stability in a wide range from 100 to 600 K [1–5]. The higher dielectric constant means the smaller size of electronics items we can have. So CCTO could be used to develop the new generation of multilayer ceramic capacitors. However, the dielectric constant of CCTO is greatly different from the calculated value ($\varepsilon_r = 49$) by first-principles method [6], the origin of giant dielectric response for CCTO was still unclear. The internal barrier layer capacitor (IBLC) model was wildly accepted to explain the anomaly of calculation and experiment. According to this model, grain boundaries which have larger resistivity than grains act as internal charge transport barriers along the electrical current percolation path and induce the high capacity [7, 8], which maybe the main reason to generate giant dielectric constant.

Usually, the high dielectric constant of CCTO accompanies a high dielectric loss [9–11]. By now, the high dielectric loss is the most serious problems preventing the use of CCTO in capacitor applications, many researchers devote to improve dielectric properties for applications. According to the IBLC model, the dielectric properties of CCTO were sensitive to the microstructure. Such as grain size, vacancies, second phase and etc. would seriously affect the electrical properties of grains and grain boundaries. Thus, doping was a useful method to modify the microstructure, which can improve the dielectric properties of CCTO ceramics in various degrees. For example, the grain size became larger with the increment of Mg²⁺ dopant concentration, which resulted in the increase of dielectric constant and the nonlinear coefficient [12, 13]. Singh [14–18] provided a sol–gel method to prepare Zn²⁺ doped CCTO ceramics with relatively low dielectric loss. The grains of Zn²⁺ doped CCTO samples were small and homogeneous, but these samples still had higher dielectric constant than un-doped CCTO. The electron concentration of CCTO/Al₂O₃ ceramic could be controlled by Al³⁺, and the change of resistivity of grains/grain boundaries could

✉ Yiming Zeng
zengym0871@126.com

[1] State Key Laboratory of Advanced Technologies for Comprehensive Utilization of Platinum Metals, Kunming Institute of Precious Metals, Kunming 650106, People's Republic of China

[2] Aerospace Science and Industry Wuhan Magnetism-electron Co., LTD, Wuhan 430074, People's Republic of China

[3] State Key Laboratory of Electronic Thin Films and Integrated Devices, University of Electronic Science and Technology of China, Chengdu 610054, People's Republic of China

improve the dielectric properties obviously. [19]. Numerous studies with CCTO showed that doping could influence the microstructure, electrical properties of grains/grain boundaries, dielectric response and nonlinear current–voltage characteristics of CCTO ceramics. Such a systematic investigation will provide more understanding of the origin mechanism of giant dielectric response in CCTO ceramics.

Up to now, the effect of $Ba^{2+}$ doping on microstructure and dielectric properties of CCTO ceramics were rarely reported. In this work, the effect of the $Ba^{2+}$ doping in microstructure, dielectric properties, complex impedance and nonlinear I–V characteristic of CCTO was investigated. Moreover, considering the mechanisms involved in the IBLC model, the effect of $Ba^{2+}$ doping were discussed.

## 2 Experimental

Analytical-grade $CaCO_3$ (99 %, Sinopharm), CuO (99 %, Sinopharm), $TiO_2$ (99 %, Aladdin) and $BaCO_3$ (99 %, Sinopharm) were used as the starting materials for synthesizing CBCTO ceramics. All starting materials were mixed in a planetary ball mill for 4 h with agate balls using deionized water as dispersant. The perovskite related CBCTO phase was formed at 950 °C for 4 h by conventional solid-state reaction. Then calcined CBCTO was milled for 4 h again and sieved through 600 meshes. The dry power was pressed into disks of a half inch in diameter and 2.5 mm in thickness under 20 MPa by using 5 wt% of PVA as organic binders. The disks were sintered at 1050 °C for 8 h, then polished and coated with Ag electrode.

XRD (Panalytical X-ray diffractometer) was performed using $CuK\alpha_1$ radiation ($\lambda = 1.5406$) to study the effect of structure with different composition in range of 10–80° with step of 0.03°. The microstructure was observed by a field-emission scanning electron microscope (FE-SEM, ZEISS). The dielectric characterization was performed by precision impedance analyzer (Agilent 4294A). The current–voltage (I–V) behavior was obtained by using Radiant 609B and direct current power (Precision 10 kV HVI-SC high-voltage). The densities of calcined powder were measured by Micromeritics AccuPyc II 1340 TEC, and the densities of sintered samples were measured using Archimedes' Principle.

## 3 Result and discussion

Figure 1 shows the XRD patterns of CBCTO powders. The diffraction data obtained for all the samples could be indexed to a body-centered cubic perovskite related
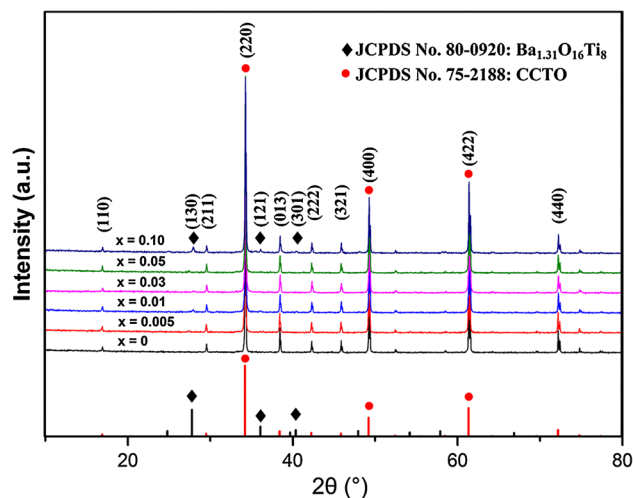


**Fig. 1** XRD patterns of references and the CCTO ceramics with different composition of x = 0, x = 0.005, x = 0.01, x = 0.03, x = 0.05 and x = 0.1

structure of space group Im3 at room temperature and the major peaks correspond to CCTO phase (JCPDS No. 75-2188). The lattice parameters of samples for x = 0, 0.005, 0.01, 0.03, 0.05 and 0.1 were calculated by HighScore plus. The values were found to be 7.3927, 7.3887, 7.3887, 7.3916, 7.3899 and 7.3905 Å, respectively. The lattice parameter of CCTO was bigger than the values of doped samples. The reported structure of CCTO is cubic perovskite with lattice parameter of 7.391 Å [5]. And the octahedral $TiO_6$ tilted to a square planar arrangement around Cu, results a small deviation of the O–Ti–O angles from 90° and Ca–O = 2.604 Å which is less than the 2.72 Å based on the ionic radii [20]. As the radius of $Ba^{2+}$ (1.42 Å) is larger than $Ca^{2+}$ (1.12 Å), $Ba^{2+}$ is hard to replace $Ca^{2+}$. In addition, the content of $Ca^{2+}$ was decreased for substitution. The absence of $Ca^{2+}$ caused the decreased of the lattice parameters. Moreover, an obvious secondary phase ($Ba_{1.31}Ti_8O_{16}$, 5 % semi-quantitative) were observed at x = 0.1. It illustrates that the solid solubility of $Ba^{2+}$ is limited and then the redundant $Ba^{2+}$ interacted with $Ti^{4+}$ and $O^{2-}$ to form the secondary phase.

Figure 2a–g shows FE-SEM images of fractured surface of all the samples, respectively. From Fig. 2a, the grain sizes of CCTO are composed with huge grains (more than 100 µm) and small particles (about 2 µm), and the grain–grain junctions by fracture can be noted. This microstructure of bimodal distribution is similar with the other reports [21]. Small holes can be noted on the huge grains, which can be attributed to the boundaries moving together during grain growing [22]. However, the CBCTO samples exhibit homogeneous grains in Fig. 2c–g. The grain size of CBCTO ceramics range from 1 to 8 µm and the polygonous grains are formed. Commonly, the sintering processing of CCTO is that the grain grown up while the Cu-
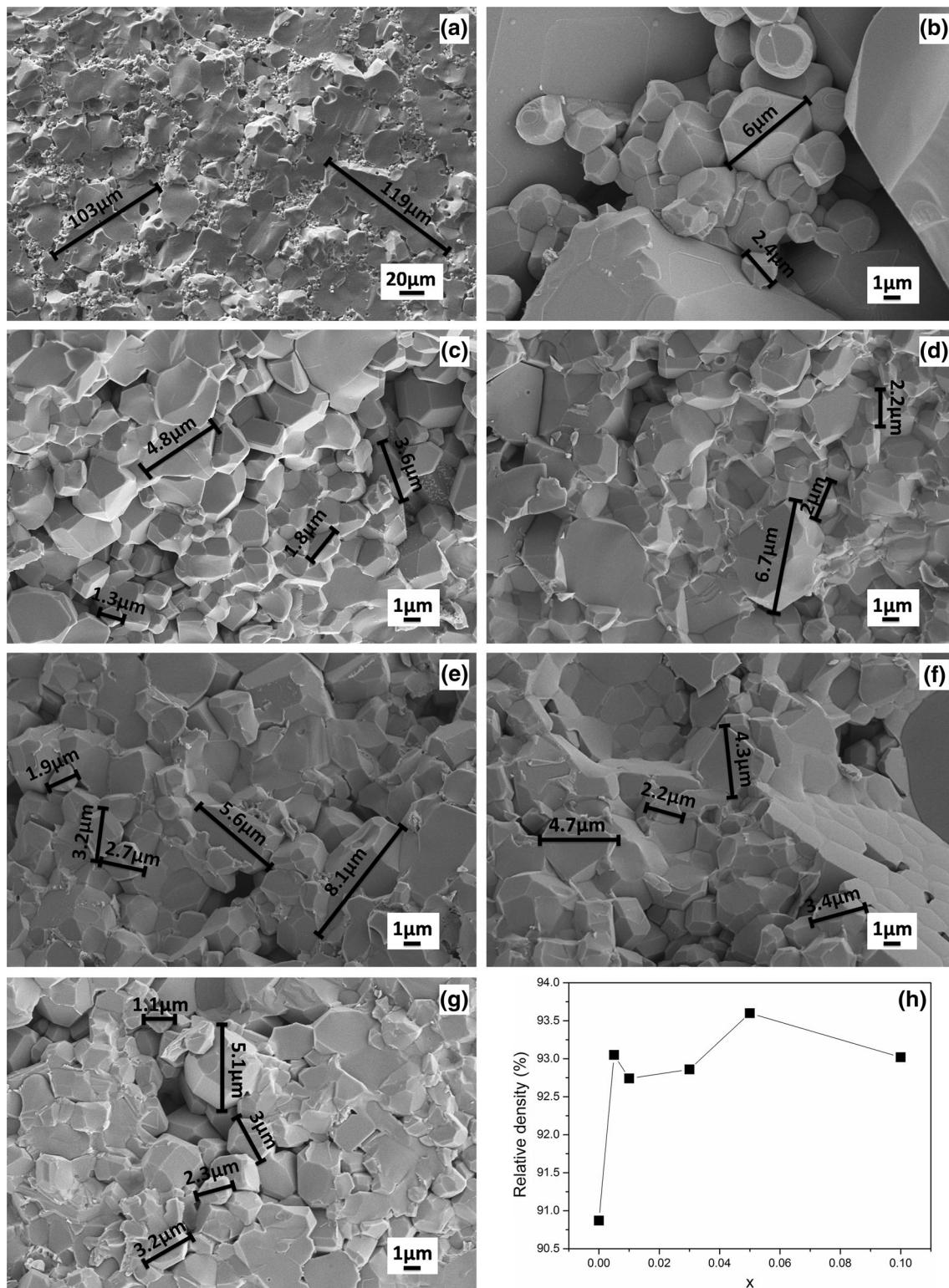
**Fig. 2** SEM micrographs of CCTO ceramics with x = 0 (**a** and **b**), x = 0.005 (**c**), x = 0.01 (**d**), x = 0.03 (**e**), x = 0.05 (**f**), x = 0.1 (**g**) and relative densities (**h**)

rich intergranular phase is formed at the grain–grain junctions to form liquid phase sintering, and then Cu come back to the lattice during the cooling processing [23–26].

According to this grain-growing mechanism, the $Ba^{2+}$ doping might restrain the forming of Cu-rich intergranular phase, and impede the movement of grain boundary. This

phenomenon is similar with $Al^{3+}$ grafted CCTO [19] and Cu-deficient CCTO [27]. In addition, it also can be seen in XRD patterns that small crests of secondary phases appearance after $Ba^{2+}$ doping. The existence of secondary phases may also impede the movement of grain boundary. Therefore, the addition of $Ba^{2+}$ inhibited grain grown and led to decreasing the grain size of CCTO, meanwhile, avoided the formation of holes too. The relative densities of samples were shown in Fig. 2h. The relative densities of CBCTO samples were higher than CCTO sample. It is revealed that the microstructural densification of CCTO ceramic increases with the decrease of hole-rate.

The frequency dependence of dielectric constant (ε) and dielectric loss (tanδ) at room temperature for the samples are shown in Fig. 3. It can be seen that the sample of CCTO had a much greater ε than other doped samples in a widely range of frequency. As many studies reported, the microstructure of CCTO which had the bimodal distribute of grain size was contributed to the giant dielectric constant of CCTO [28]. However, the doped samples have a homogeneous grain size
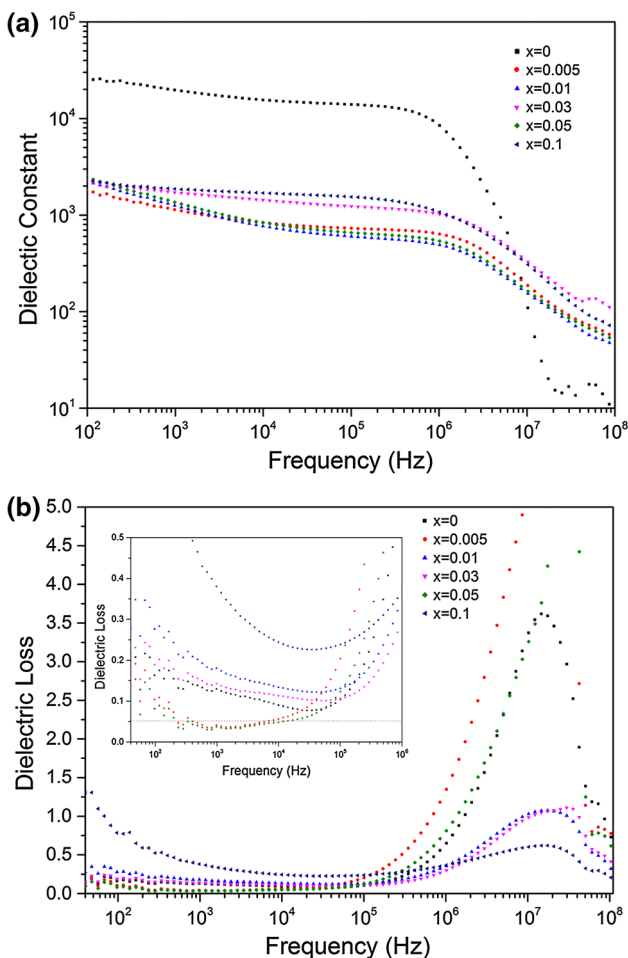


**Fig. 3** Frequency dependence of dielectric constant (**a**) and dielectric loss (**b**) of CCTO ceramics

about 4 μm, which cause the decrease of dielectric constant. It also can be observed that all the ε turn to decrease at frequency about $10^6$ Hz. The ε of CCTO rapidly decreased from $10^4$ to 10 in frequency range $10^6$ Hz to $10^8$ Hz, while that of doped samples slowly decreased from $10^3$ to 50. The results suggest that the CBCTO samples present better frequency stability than CCTO sample, which may be caused both the doping of $Ba^{2+}$ and the grain size. The variation tendencies of dielectric loss with frequency for the samples are presented in Fig. 3b. The dielectric loss of doped samples did not change much from the value of CCTO sample. According the widely accepted IBLC model, the dielectric loss before $10^5$ mainly originates from the leakage current of insulating barriers at grain boundaries [29]. As the result of the changing of the microstructure and the existing of secondary phases, the dielectric loss was not improved by $Ba^{2+}$ doping.

Impedance and modulus analysis separates the contributions of the grains and grain boundaries for the total observed resistance and capacitance of the samples, respectively. Typical complex plane impedance plot obtained for all samples are shown in Fig. 4a. The data for the impedance spectra are modeled by an ideal equivalent circuit consisting of two parallel RC components [30]. It should be noted that the resistance of grains ($R_g$) increased and the resistance of grain-boundaries ($R_{gb}$) decreased after $Ba^{2+}$ doping. As mentioned before, $Ba^{2+}$ doping might influence the processing of grain-growing. The deviation of stoichiometry might cause these changes of resistance. As shown in Fig. 4b, the $R_{gb}$ value of samples was greatly reduced after $Ba^{2+}$ doping. This result might be one reason for lower dielectric constant of $Ba^{2+}$ doped samples as compared to undoped CCTO. It was similar to the phenomenon observed in $Nb^{5+}$ and $Ta^{5+}$ doped CCTO ceramics [23, 31], which means $R_{gb}$ is sensitive to substitution. The $R_g$ value was increased from 190 to 280 Ω, which was larger than the value of CCTO sample. However, the change tendency of electric properties with $Ba^{2+}$ doping content did not present regularity. Moreover, the small grains of doped samples meant that the ratio of grain boundaries increased, but the resistance reduced. According to the IBLC model, the grain boundary as the internal charge transport barrier mightily influenced the properties of CCTO.

All the samples present good nonlinear current–voltage (I–V) behavior and good electrical breakdown field ($E_b$) from Fig. 5. The $E_b$ values of the x = 0, 0.005, 0.01, 0.03, 0.05 and 0.1 samples were 1.5, 7.4, 5.8, 22.4, 2.76 and 8 kV/cm, respectively. The coefficient of nonlinearity was calculated by the equation as follow [32]:
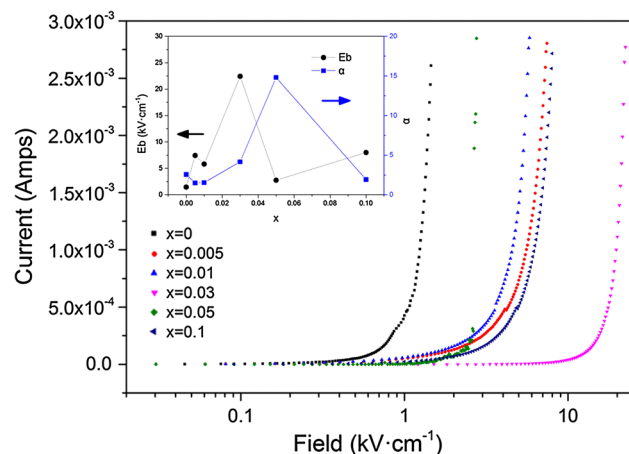
$$I = KV^\alpha \qquad (1)$$

where K is a constant related to the electrical resistivity of the material. And α was the nonlinear coefficient which
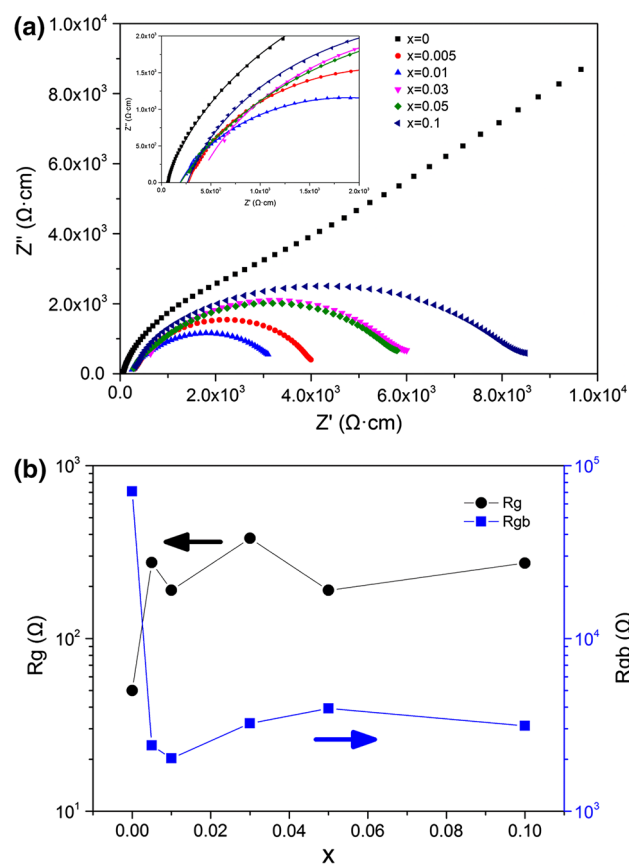
Fig. 4 Impedance complex plane plot (a) and resistance of grain/grain boundary (b) of CCTO ceramics



Fig. 5 Current-voltage characteristics of CCTO ceramics

**Table 1** Nonlinear coefficient ($\alpha$) and breakdown field ($E_b$) of CCTO ceramics

| sample | $\alpha$ | $E_b$ |
|---|---|---|
| $Ca_{1-x}Ba_xCu_3Ti_4O_{12}$ | | |
| x = 0 | 2.56 | 1.5 |
| x = 0.005 | 1.5 | 7.4 |
| x = 0.01 | 1.54 | 5.8 |
| x = 0.03 | 4.17 | 22.4 |
| x = 0.05 | 14.81 | 2.76 |
| x = 0.1 | 1.71 | 8 |
| CCTO [33] | 5.85 | 3.27 |
| CCTO-Y [34] | 1.98 | 0.99 |
| CCTO-La [34] | 1.67 | 0.89 |
| CCTO-Eu [34] | 2.56 | 6.41 |
| CCTO-Gd [34] | 2.38 | 4.56 |
| CCTO-NiO [35] | 3.66 | 0.32 |
| CCTO-SnO$_2$ [35] | 3.77 | 0.49 |
| CCTO-SiO$_2$ [35] | 2.75 | 0.3 |
| CCTO-Al$_2$O$_3$ [35] | 3.74 | 1.39 |

hand, $Ba^{2+}$ doping decreased the resistance of grain boundary. The $\alpha$ and $E_b$ should be lower than the value of pure CCTO. On the other hand, small grain size meant more grain boundary in samples. The doped samples should have better $\alpha$ and $E_b$ than CCTO. The combined action of grain size and electric properties of grain boundary caused that $Ba^{2+}$ doped samples which still had good nonlinear I–V behavior with obviously fluctuation data of $\alpha$ and $E_b$.

## 4 Conclusion

$Ca_{1-x}Ba_xCu_3Ti_4O_{12}$ (CBCTO) ceramics were prepared by two-step solid state reaction method. The results showed that little amount of secondary phases were existed in CBCTO ceramics from the XRD analysis. The dielectric constant of the samples decreased with $Ba^{2+}$ substitution, but exhibited better frequency dependence stability than CCTO sample. As the result of $Ba^{2+}$ doping, grains showed small and homogeneous microstructure, and the resistance of grain-boundary decreased. The combined action of the change of resistance and grain size caused the decrease of dielectric constant. In this regard, the present results suggest that $Ba^{2+}$ can be used to regulate and control the microstructure and the properties of CCTO.

was calculated in the range of $J = 10^{-4}$–$10^{-3}$ A/cm$^2$. The $\alpha$ and $E_b$ values of $Ba^{2+}$ doped CCTO and the values from other studies were listed in table 1. Compare with the results of them, Ba2+ doping could significantly enhance the breakdown field of CCTO. The variations of $\alpha$ and $E_b$ should be associated with the grain boundaries. On one

# References

1. A.P. Ramirez, M.A. Subramanianb, M. Gardel, G. Blumberg, D. Li, T. Vogt, S.M. Shapiro, Giant dielectric constant response in a copper-titanate. Solid State Commun. **115**, 217–220 (2000)

2. P. Liu, Y.M. Lai, Y.M. Zeng, S. Wu, Z.H. Huang, J. Han, Influence of sintering conditions on microstructure and electrical properties of $CaCu_3Ti_4O_{12}$ (CCTO) ceramics. J. Alloys Compd. **650**, 59–64 (2015)

3. C.C. Homes, T. Vogt, S.M. Shapiro, S. Wakimoto, A.P. Ramirez, Optical response of high-dielectric-constant perovskite-related oxide. Science **293**, 673–676 (2001)

4. T.T. Fang, H.K. Shiau, Mechanism for developing the boundary barrier layers of $CaCu_3Ti_4O_{12}$. J. Am. Ceram. Soc. **87**, 2072–2079 (2004)

5. M.A. Subramanian, D. Li, N. Duan, B.A. Reisner, A.W. Sleight, High dielectric constant in $ACu_3Ti_4O_{12}$ and $ACu_3Ti_3FeO_{12}$ phases. J. Solid State Chem. **151**, 323–325 (2000)

6. L. He, J.B. Neaton, M.H. Cohen, D. Vanderbilt, C.C. Homes, First-principles study of the structure and lattice dielectric response of $CaCu_3Ti_4O_{12}$. Phys. Rev. B Condens. Matter **65**, 214112 (2002)

7. D.C. Sinclair, T.B. Adams, F.D. Morrison, A.R. West, $CaCu_3Ti_4O_{12}$: One-step internal barrier layer capacitor. Appl. Phys. Lett. **80**, 2153 (2002)

8. T.B. Adams, D.C. Sinclair, A.R. West, Giant barrier layer capacitance effects in $CaCu_3Ti_4O_{12}$ ceramics. Adv. Mater. **14**, 1321–1323 (2002)

9. P. Mishra, P. Kumar, Structural, dielectric and optical properties of [(BZT–BCT)-epoxy-CCTO)] composites. Ceram. Int. **41**, 2727–2734 (2015)

10. R. Xue, Z. Chen, H. Dai, D. Liu, T. Li, G. Zhao, Effects of rare earth ionic doping on microstructures and electrical properties of $CaCu_3Ti_4O_{12}$ ceramics. Mater. Res. Bull. **66**, 254–261 (2015)

11. W. Wan, C. Liu, H. Sun, Z. Luo, W.X. Yuan, H. Wu, T. Qiu, Low-toxic gelcasting of giant dielectric-constant $CaCu_3Ti_4O_{12}$ ceramics from the molten salt powder. J. Eur. Ceram. Soc. **35**, 3529–3534 (2015)

12. M.F.A. Rahman, J.J. Mohamed, M.F. Ain, S.D. Hutagalung, The effect of MgO dopant on the dielectric properties of $CaCu_3Ti_4O_{12}$ ceramics. Adv. Mater. Res. **620**, 219–223 (2012)

13. J. Jumpatam, B. Putasaeng, T. Yamwong, P. Thongbai, S. Maensiri, A novel strategy to enhance dielectric performance and non-Ohmic properties in $Ca_2Cu_{2-x}Mg_xTi_4O_{12}$. J. Eur. Ceram. Soc. **34**, 2941–2950 (2014)

14. L. Singh, U.S. Rai, K.D. Mandal, Influence of Zn doping on microstructures and dielectric properties in $CaCu_3Ti_4O_{12}$ ceramic synthesised by semiwet route. Adv. Appl. Ceram. **111**(7), 374–380 (2012)

15. L. Singh, U.S. Rai, K.D. Mandal, M. Yashpal, Dielectric properties of ultrafine Zn-doped $CaCu_3Ti_4O_{12}$ ceramic. J. Adv. Dielectr. **02**, 1250007 (2012)

16. L. Singh, U.S. Rai, K.D. Mandal, Dielectric properties of zinc doped nanocrystalline calcium copper titanate synthesized by different approach. Mater. Res. Bull. **48**(6), 2117–2122 (2013)

17. L. Singh, U.S. Rai, A.K. Rai, K.D. Mandal, Sintering effects on dielectric properties of Zn-doped $CaCu_3Ti_4O_{12}$ ceramic synthesized by modified sol–gel route. Electron. Mater. Lett. **9**(1), 107–113 (2013)

18. L. Singh, I.W. Kim, B.C. Sin, K.D. Mandal, U.S. Rai, A. Ullah, H. Chung, Y. Lee, Dielectric studies of a nano-crystalline $CaCu_{2.90}Zn_{0.10}Ti_4O_{12}$ electro-ceramic by one pot glycine assisted synthesis from inexpensive $TiO_2$ for energy storage capacitors. RSC Adv **4**(95), 52770–52784 (2014)

19. A. Rajabtabar-Darvishi, R. Bayati, O. Sheikhnejad-Bishe, L.D. Wang, W.L. Li, J. Sheng, W.D. Fei, Giant dielectric response and low dielectric loss in $Al_2O_3$ grafted $CaCu_3Ti_4O_{12}$ ceramics. J. Appl. Phys. **117**(9), 094103 (2015)

20. R.D. Shannon, Revised effective ionic radii and systematic studies of interatomic distances in halides and chalcogenides. Acta Crystallogr. Sect. A Found. Crystallogr. **32**, 751–767 (1976)

21. L.F. Xu, P.B. Qi, X.P. Song, X.J. Luo, C.P. Yang, Dielectric relaxation behaviors of pure and $Pr_6O_{11}$-doped $CaCu_3Ti_4O_{12}$ ceramics in high temperature range. J. Alloys Compd. **509**, 7697–7701 (2011)

22. Arunachalam Lakshmanan, *Sintering of ceramics–new emerging techniques* (InTch, Croatia, 2012)

23. P. Thongbai, J. Jumpatam, T. Yamwong, S. Maensiri, Effects of $Ta^{5+}$ doping on microstructure evolution, dielectric properties and electrical response in $CaCu_3Ti_4O_{12}$ ceramics. J. Eur. Ceram. Soc. **32**, 2423–2430 (2012)

24. J. Jumpatam, B. Putasaeng, T. Yamwong, P. Thongbai, S. Maensiri, Enhancement of giant dielectric response in Ga-doped $CaCu_3Ti_4O_{12}$ ceramics. Ceram. Int. **39**, 1057–1064 (2013)

25. P. Leret, J.F. Fernandez, J. de Frutos, D. Fernández-Hevia, Nonlinear I–V electrical behaviour of doped CaCu3Ti4O12 ceramics. J. Eur. Ceram. Soc. **27**, 3901–3905 (2007)

26. L. Liu, D. Shi, S. Zheng, Y. Huang, S. Wu, Y. Li, L. Fang, C. Hu, Polaron relaxation and non-ohmic behavior in $CaCu_3Ti_4O_{12}$ ceramics with different cooling methods. Mater. Chem. Phys. **139**(2–3), 844–850 (2013)

27. L. Liu, H. Fan, X. Chen, P. Fang, Electrical properties and microstructural characteristics of nonstoichiometric $CaCu_{3x}Ti_4O_{12}$ ceramics. J. Alloys Compd. **469**(1–2), 529–534 (2009)

28. S.D. Hutagalung, L.Y. Ooi, Z.A. Ahmad, Improvement in dielectric properties of Zn-doped $CaCu_3Ti_4O_{12}$ electroceramics prepared by modified mechanical alloying technique. J. Alloys Compd. **476**, 477–481 (2009)

29. T.T. Fang, H.Y. Chung, Reassessment of the impedance spectra and dielectric responses of undoped and $CaSiO_3$-doped $CaCu_3Ti_4O_{12}$. J. Appl. Phys. **109**, 014102 (2011)

30. A.R. West, T.B. Adams, F.D. Morrison, D.C. Sinclair, Novel high capacitance materials: $BaTiO_3$: La and $CaCu_3Ti_4O_{12}$. J. Eur. Ceram. Soc. **24**, 1439–1448 (2004)

31. P. Liu, Y. He, J.P. Zhou, C.H. Mu, H.W. Zhang, Dielectric relaxation and giant dielectric constant of Nb-doped $CaCu_3Ti_4O_{12}$ ceramics under dc bias voltage. Phys. Status Solidi A **206**, 562–566 (2009)

32. D.R. Clarke, Varistor ceramics. J. Am. Ceram. Soc. **82**, 485–502 (1999)

33. Y. Huang, D. Shi, Y. Li, G. Li, Q. Wang, L. Liu, L. Fang, Effect of holding time on the dielectric properties and non-ohmic behavior of $CaCu_3Ti_4O_{12}$ capacitor-varistors. J. Mater. Sci. Mater. Electron. **24**(6), 1994–1999 (2012)

34. L. Liu, L. Fang, Y. Huang, Y. Li, D. Shi, S. Zheng, S. Wu, C. Hu, Dielectric and nonlinear current–voltage characteristics of rare–earth doped $CaCu_3Ti_4O_{12}$ ceramics. J. Appl. Phys. **110**(9), 094101 (2011)

35. L. Liu, Y. Huang, Y. Li, D. Shi, S. Zheng, S. Wu, L. Fang, C. Hu, Dielectric and non-Ohmic properties of $CaCu_3Ti_4O_{12}$ ceramics modified with NiO, $SnO_2$, $SiO_2$, and $Al_2O_3$ additives. J. Mater. Sci. **47**(5), 2294–2299 (2011)